Impact of Grid-Connected Doubly-Fed Induction Wind Generators on Voltage Stability

Ce Zheng, *Student Member, IEEE*, and Mladen Kezunovic, *Fellow, IEEE*

***Abstract*--The increase of installed capacity of wind generation influences the nodal voltages of existing electric power systems. This paper investigates the dynamic behavior of Doubly-fed Induction Wind Generators (DFIWG) and their impacts on system voltage stability. The dynamic analysis is conducted by initializing and integrating wind generator variables involved in the load flow calculation. Large disturbance voltage stability is then examined considering a major system fault as well as the subsequent actions of On-Load Tap Changer (OLTC). The small disturbance voltage stability analysis is performed by monitoring the distribution of critical eigenvalues under the variation of wind speed. The voltage/VAR support provided by DFIWG is quantified through sensitivity analysis of the critical eigenvalue variation versus the adjustment of DFIWG controller parameters. A deeper understanding of the system voltage stability issues is obtained by extending the eigenvalue analysis to a 23-bus system.**

***Index Terms*—Doubly-fed induction wind generator, voltage stability, small disturbance, sensitivity, eigenvalue analysis**

I. Introduction

With the unprecedented world-wide expansion of wind power generation both in size and in capacity, traditional power systems are exposed to new challenges. Among them, two very important issues have drawn great attention: (a) the variable-speed wind generators exhibits novel dynamic behaviors that need to be better understood; (b) the development of wind generation leads to increased power transfers and reduced transmission margins which have significant impacts on system voltage stability.

Voltage stability as defined in [1] has been extensively studied around 1990s. At that time, most of the researches are focused on the ability of synchronous generators to maintain acceptable voltage levels [2]. From the end of the last century, the wind generators based on fixed-speed wind turbines have been included in stability studies [3]-[4]. Recently, with the increasing market share of variable-speed wind generators, the grid stability enhancement of variable-speed wind generators, especially the Doubly-Fed Induction Wind Generators (DFIWG), has been reported in several publications [5]-[6].

The concern of voltage stability can be further classified into large disturbance and small disturbance categories. The large disturbance voltage stability analysis examines the voltage behavior of a system under a major disturbance, e.g. a system fault. On the other hand, the small disturbance voltage stability refers to the system's ability to maintain steady voltage levels following small disturbances, e.g. a variation in load.

While the concern of small disturbance stability is on the continuous variations in load [7], with the expansion of wind generation, operational uncertainty will extend from demand side variability to a significant portion of the supply side variability as well. Reference [8] and [9] conducted modal analysis to investigate the intrinsic dynamics of grid-connected DFIWG. While their focus is on the small-signal stability, the issue of small disturbance voltage instability induced by the fluctuation of wind power outputs is hitherto largely ignored.

This paper discusses three different yet closely correlated aspects of the voltage stability issue under the new energy transfer scenario where traditional generators are supplanted by wind generators. It begins with a comparison of the dynamic models for fixed/variable-speed wind generators. The parameter initialization of DFIWG dynamic model is then introduced. The voltage stability of a test system has been scrutinized under two situations: (1) system fault; (2) wind speed variation. The voltage performance in the presence of a local DFIWG-based wind farm is studied considering a system fault as well as the subsequent actions of a mechanical OLTC. After that, small disturbance voltage stability analysis is performed by reducing system state space equations and tracking the eigenvalue movement with slow variations of wind farm output. Finally, the voltage/VAR support provided by DFIWG is analyzed by monitoring the critical eigenvalue variation versus the adjustment of DFIWG reactive power controller's parameters.

It is found that the reactive power controller's parameters have considerable impact on the trajectory of critical eigenvalues. A deeper understanding of the small disturbance voltage stability has been obtained through eigenvalue analysis of a 23-bus system. Voltage stability enhancement is quantified based on the sensitivity assessment.

The paper is organized as follows. Section II provides circuit analysis and variable initialization process for DFIWG. Section III investigates the large disturbance voltage stability of a test system with wind farm connected. It is followed by the small disturbance voltage stability analysis which is conducted in Section IV. In Section V, the trajectory sensitivity analysis is performed. The conclusions are given at the end.

Ce Zheng and Mladen Kezunovic are with the Department of Electrical and Computer Engineering, Texas A&M University, College Station, TX 77840 USA (e-mails: zhengce@neo.tamu.edu; kezunov@ece.tamu.edu).

II. Background

The wind generator models and their equivalent circuits are formulated for: (1) Fixed-speed Squirrel Cage Induction Wind Generators (SCIWG); (2) Variable-speed wind generation system represented by DFIWG.

A. Circuit Analysis of SCIWG

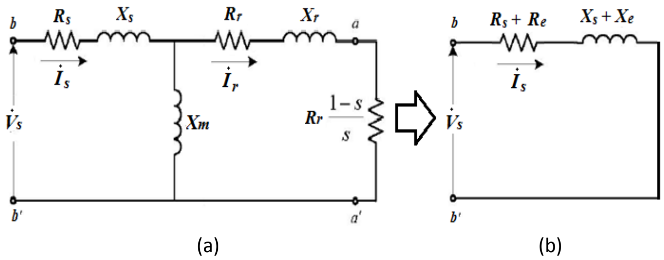

Fig. 1. Steady-state equivalent circuit of SCIWG and its Thevenin equivalent

When rotor electrical transients have died out, the SCIWG can be represented by the well-known steady-state equivalent circuit shown in Fig. 1(a).

In the Thevenin equivalent shown in Fig. 1(b), slip s, R_e and X_e are (stator resistance is neglected):

$$\begin{cases} s = \frac{\omega_0 - \omega_r}{\omega_0} \\ R_e = \frac{R_r X_m^2}{s\left[\left(\frac{R_r}{s}\right)^2 + (X_m + X_r)^2\right]} \\ X_e = \frac{X_m\left[R_r^2 + s^2 X_r (X_m + X_r)\right]}{R_r^2 + s^2 (X_m + X_r)^2} \end{cases} \tag{1}$$

The stator current is thus calculated as:

$$\vec{I_s} = \frac{\vec{V_s}}{(R_s + R_e) + j(X_s + X_e)} \tag{2}$$

B. Circuit Analysis of DFIWG

The steady-state and dynamic equivalent circuits of DFIWG are given by Fig. 2.

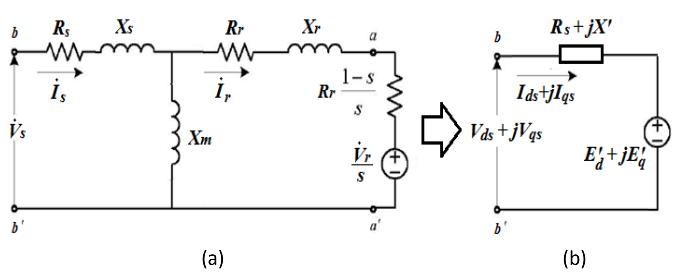

Fig. 2. DFIWG steady-state and dynamic equivalent circuits

The dynamic variables in Fig. 2(b) are calculated as:

$$\vec{E}_{eq} = E_d' + jE_q' = \frac{jX_m \frac{\vec{V_r}}{s}}{\frac{R_r}{s} + j(X_m + X_r)} \tag{3}$$

$$R_s + jX' = R_s + jX_s + \frac{jX_m\left(\frac{R_r}{s} + jX_r\right)}{\frac{R_r}{s} + j(X_m + X_r)} \tag{4}$$

$$I_{ds} + jI_{qs} = \frac{V_{ds} + jV_{qs} - \vec{E}_{eq}}{R_s + jX'} \tag{5}$$

C. Initialization of Internal Variables

According to Fig. 2(b), the dynamic model of DFIWG can be describes as below:

$$\begin{cases} V_{qs} = E_q' - R_s I_{qs} - X_s' I_{ds} \\ V_{ds} = E_d' - R_s I_{ds} + X_s' I_{qs} \\ I_{qr} = -\frac{E_{dD}'}{X_m} + \frac{X_m}{X_r} I_{qs} \\ I_{dr} = \frac{E_q'}{X_m} + \frac{X_m}{X_r} I_{ds} \\ \frac{2H}{\omega_s}\frac{d\omega_r}{dt} = T_m - E_d' I_{ds} - E_q' I_{qs} \end{cases} \tag{6}$$

When connected to the grid, the involved internal variables should be initialized at each operating point (OP) before performing time-domain and frequency-domain analysis [10]. The initialization is conducted by incorporating the wind farm at its Point of Interconnection (POI) into the power flow analysis to get a 'snapshot' of current OP. Fig. 3 shows the process deployed to initialize the DFIWG internal variables:

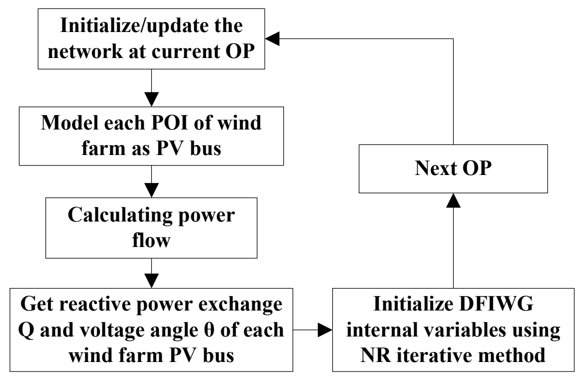

Fig. 3. DFIWG internal variables initialization procedure

III. Voltage Stability Under System Fault

In this section, voltage stability is examined under system fault using the time-domain calculation. The subsequent actions of OLTC are considered.

A. Description of the Examined System

The examined system is shown in Fig. 4. A local wind farm is equipped with 25 DFIWGs, each having a capacity of 3.6 MW. It is connected to Bus 2 through a step-up transformer *T1*. Load is fed by the local wind farm and external network through an OLTC transformer at Bus 3. Most of the electric power is provided by the external network through a double-circuit transmission line between Bus 1 and Bus 2.

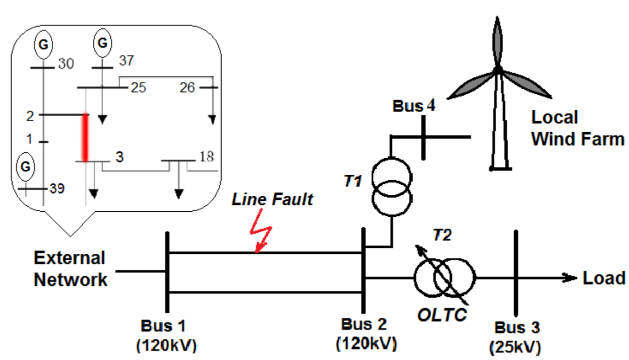

Fig. 4. One-line diagram of the four-bus test system

A three-phase fault has induced the tripping of one transmission line between Bus 1 and Bus 2.

The Thevenin-like equivalent model of the test system, as seen from the load bus, is shown in Fig.5.

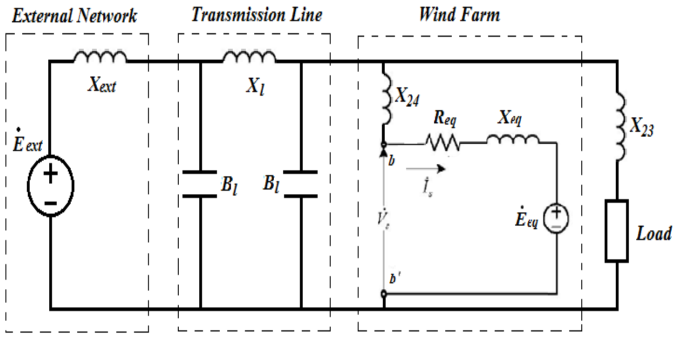

Fig. 5. Circuit representation of the test system

Network equations include the generator equations, power flow equations, and representation of loads. OLTC is included in the power flow equations. The load at Bus 3 is modeled as constant MVA load.

For network load flow, the well known equations in terms of real and reactive powers are deployed:

$$P_i - V_i \sum_{j \in N} V_j [G_{ij} \cos(\theta_i - \theta_j) + B_{ij} \sin(\theta_i - \theta_j)] = 0 \quad (7)$$

$$Q_i - V_i \sum_{j \in N} V_j [B_{ij} \cos(\theta_i - \theta_j) - G_{ij} \sin(\theta_i - \theta_j)] = 0 \quad (8)$$

where i, j represent bus number, and N is the total number of network nodes.

Taking into account the models of step-up transformer $T1$ and the OLTC, the admittance between Bus 2 and Bus 4, as well as between Bus 2 and Bus 3 are detailed as follows:

$$B_{ij} = -\frac{1}{nX_{ij}}, \quad B_{sij} = \frac{1-n}{nX_{ij}}, \quad B_{sji} = \frac{n-1}{n^2 X_{ij}} \quad (9)$$

where $i = 2,\ \ j = 3, 4,\ \ n$ is the transformer turns ratio, and B_s is the self admittance.

The load has been modeled as exponential load with the following characteristics:

$$P = P_0 (\frac{V_3}{V_{30}})^{\alpha}, \quad Q = Q_0 (\frac{V_3}{V_{30}})^{\beta} \quad (10)$$

where V_{30} is the reference voltage magnitude at Bus 3, and the exponents α and β depend on the type of the load. The load will have constant power factor as long as $\alpha = \beta$.

B. Voltage Stability Analysis

DFIWG could provide reactive power to the external grid and may provide voltage support. Simulation verification of this assertion has been described in [11]-[12]. We will examine the impact of DFIWG on grid voltage from another aspect, where subsequent actions of OLTC are considered.

The Bus 2 voltage magnitude and corresponding real power feeding the load is calculated in time-domain. A set of equilibrium equations needs to be solved. The wind generator equations listed in (1)-(6) together with the network equations listed in (7)-(10) are included. To obtain the large portions of the power-voltage curve, the range of variation of the OLTC turns ratio n has been extended. The specific values of system parameters used in the calculation are detailed in Appendix A.

The tripping of one line induces a reduced transfer capability between Bus 2 and the external network, which leads to a decrease of the maximum loadability.

The Bus 3 long-term voltage stability is then analyzed. The three-phase fault is applied to one transmission line between Bus 1 and Bus 2 at t = 8 s. The Bus 3 voltage magnitude is calculated and recorded in Fig. 6.

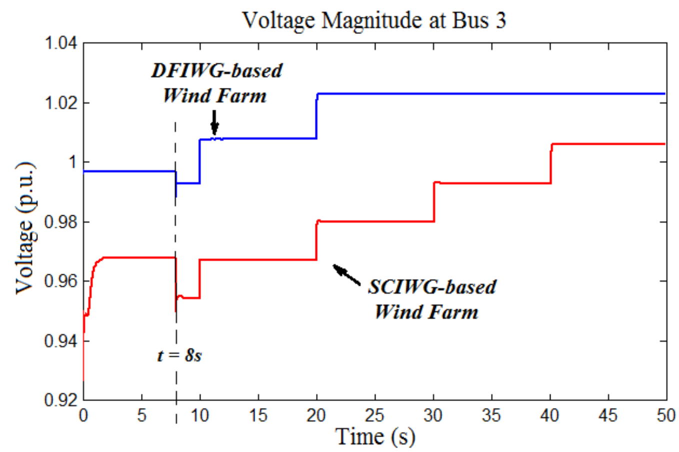

Fig. 6. Voltage magnitude at Bus 3 in the presence of different wind farms

It can be observed from Fig. 6 that before and after the fault, the load bus voltage magnitude is closer to its acceptable value in the presence of DFIWG-based wind farm, and hence requires less OLTC tap changes to get the voltage level back to normal. It can be concluded that DFIWG-based wind farm enables a better voltage performance, thus supports an increased real power transfer capability.

IV. SMALL DISTURBANCE VOLTAGE STABILITY

While the voltage stability analysis conducted in the previous section assumed a major disturbance has occurred, this section will further explore the small disturbance voltage instability caused by the slow variation in wind generation. This kind of voltage stability is usually evaluated by static analysis tools while it essentially has dynamic nature.

The behavior of the test system shown in Fig. 4 could always be described by a set of state-space Differential Algebraic Equations (DAE):

$$\dot{x} = f_x x + f_y y \quad (11)$$

$$0 = g_x x + g_y y \quad (12)$$

where x represents system state variables and y represents the control variables, f_x, f_y, g_x and g_y are system state matrices.

When the wind farm output, primarily determined by wind speed, is slowly changing, the non-linear differential equations can be linearized around each OP. This is suitable for conducting small disturbance analysis.

Traditional small-signal stability analysis linearizes the system at each OP and analyzes the matrix J_G:

$$\Delta\dot{x} = (f_x - f_y {g_y}^{-1} g_x) \Delta x = J_G \Delta x \quad (13)$$

We are concerned about the voltage stability in this paper. By assuming all involved dynamic state variables are at their equilibrium points, which is reasonable in SD voltage stability analysis, the matrix J_L instead of J_G will be analyzed:

$$0 = \left(g_y - g_x {f_x}^{-1} f_y\right)\Delta y = J_L \Delta y \qquad (14)$$

The matrix J_L provides a linearization around the system equilibrium point and is formulated from system DAE. The system DAE is detailed by dynamic modeling of each network component.

A. DAE of DFIWG and Other Network Components

A decoupled PQ control is assumed and the Voltage/VAR control is realized by controlling the d-axis rotor voltage through DFIWG reactive power controller. The DFIWG reactive power controller adopted in this work is represented in Fig. 7:

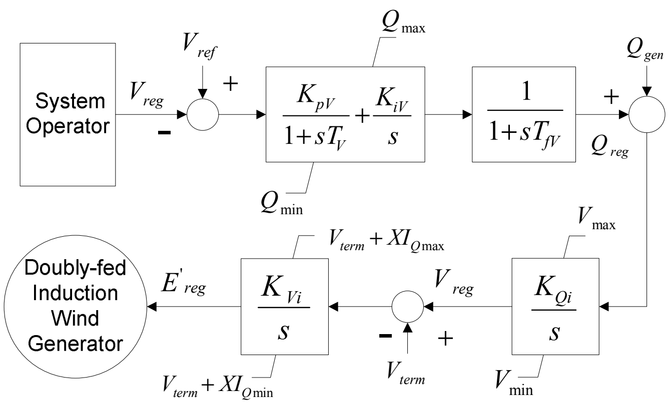

Fig. 7. DFIWG reactive power controller

From (6) and Fig. 7, the differential equations of DFIWG are derived and listed in (15):

$$\begin{cases} \dot{E_q'} = -\frac{1}{T_0'}\left[E_q' + (X_s - X_s')I_{ds}\right] + \\ \qquad \left[\omega_s \frac{X_m}{X_r} V_{dr} - (\omega_s - \omega_r)E_d'\right] \\ \dot{E_d'} = -\frac{1}{T_0'}\left[E_d' + (X_s - X_s')I_{qs}\right] + \\ \qquad \left[-\omega_s \frac{X_m}{X_r} V_{qr} + (\omega_s - \omega_r)E_q'\right] \\ \dot{\omega_r} = \frac{\omega_s}{2H}\left(T_m - E_d' I_{ds} - E_q' I_{qs}\right) \end{cases} \qquad (15)$$

The definition of the state variables and parameters included in (15) could be found in [3]. For the shaft system, the two-mass representation detailed in [13] is adopted in this work. Also, the algebraic equations of DFIWG are derived.

Similarly, the DAE for the rest of the system, such as synchronous machines, other types of generators, system load, and power flow equations can be obtained. By combining the network DAE with the set of DFIWG DAE, the overall sets of state variables x, control variables y, as well as state matrices f_x, f_y, g_x and g_y in (11) and (12) could have been formulated.

B. Small Disturbance Voltage Stability Analysis

The small disturbance (SD) voltage stability analysis essentially monitors the eigenvalue trajectory of the matrix J_L in (14). For a given wind generation level, using the state matrices formulated in the previous steps, a system Jacobian J_L can be uniquely determined. Calculating the eigenvalues of the system Jacobian matrix, the SD voltage stability can be monitored by checking if all the eigenvalues are located on the left half of the complex plane. Then, by slowly varying the real power generation of DFIWGs, the critical voltage stability point is identified when one of the eigenvalues reaches imaginary axis. If it is a pair of complex eigenvalues who first crosses the imaginary axis, this critical voltage stability point will reflect on the Power-Voltage (PV) curve as the well-known Hopf Bifurcation point.

When the SD voltage stability analysis is applied to a system with wind farm connected, the real part of critical eigenvalues Eig_{real} should be discussed differently as the way the mechanical power of a wind generator is divided. Although the wind speed is continuously distributed, the mechanical power output of wind generator is applied in a discrete manner according to the cut-in, rated and cut-out wind speeds. Consequently, the system response Eig_{real} should be modeled as:

$$Eig_{real} = \begin{cases} P_1(v_{wind}) & S1{:}\ v_{wind} < v_{in};\ v_{out} < v_{wind} \\ P_2(v_{wind}) & S2{:}\ v_{in} \le v_{wind} < v_{rated} \\ P_3(v_{wind}) & S3{:}\ v_{rated} \le v_{wind} < v_{out} \end{cases} \qquad (16)$$

In this research, the cut-in, cut-out and rated wind speeds are specified as 4 m/s, 20.9 m/s and 12.9 m/s respectively. The eigenvalue analysis is conducted using the commercial software MATLAB and PSS/E [14]. The calculation of critical eigenvalues is detailed in Appendix B.

The loci of Eig_{real} with the variation of v_{wind} under the situation of $S2$ are calculated and plotted in Fig. 8.

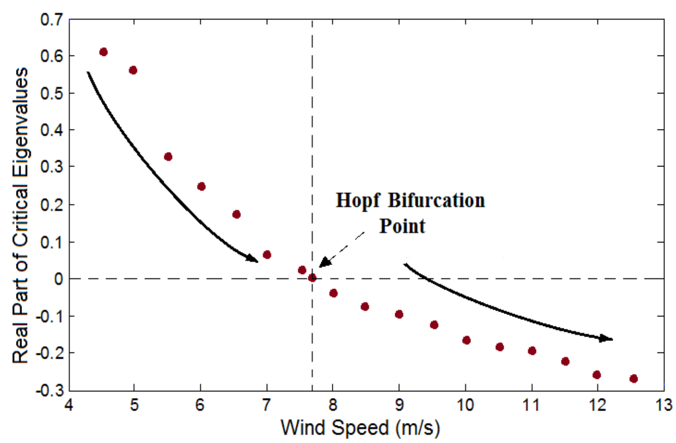

Fig. 8. Loci of Eig_{real} with the variation of v_{wind} in situation $S2$

The probability density function (PDF) of a wind plant power outputs can be summarized from the historical data. Knowing the PDF of wind generation, the probabilistic distribution of critical eigenvalues could be obtained by means of simulation-based method.

In this work, the Monte Carlo method is applied using 5000 samples and 10000 samples respectively. Assume the wind generation exhibits a Gaussian distribution. Fig. 9 shows the simulation results of the probabilistic eigenvalue distribution under the situation of S2.

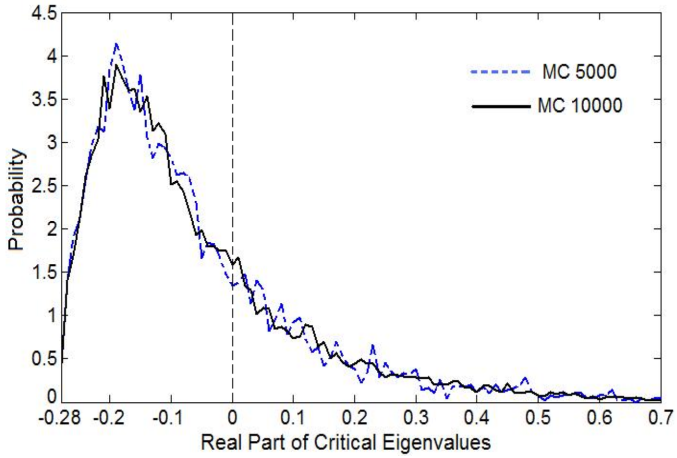

Fig. 9. Calculated probabilistic distribution of Eig_{real} under the situation of $S2$ using Monte Carlo method

In Fig. 9, the area located on the left half of the complex plane indicates that the voltage is SD stable. The integral of this stable area could be used to represent the probability of SD voltage stability under current operation point.

V. Parameter Sensitivity Analysis

A. Trajectory Sensitivities

The concept of trajectory sensitivity is not new [15]-[16]. It describes the changes in the trajectory of outputs resulting from perturbations in the underlying parameters and/or initial conditions (inputs). This could also be understood as the small changes in inputs map through the linearized relationship to small output changes. Trajectory sensitivity analysis provides a basis for ranking the relative influence of parameters. Large sensitivities imply that parameter variations have a large effect on system dynamic behavior and vice versa.

B. Voltage/VAR Support from DFIWG

Grid-connected DFIWG can provide voltage/VAR support. In this work, we quantify the voltage stability enhancement in terms of the trajectory sensitivity of critical eigenvalue to the adjustment of DFIWG controller's parameters. The parameters of reactive power control loop have been treated in particular because they directly influence the VAR exchange between the DFIWG-based wind farm and the external grid.

To reveal the above relationship in a quantitative manner, an intensive sensitivity calculation has been performed. The test system shown in Fig. 4 is used to conduct the analysis. The variation of critical eigenvalues $\lambda = \sigma \pm j\omega$ with the perturbations of K_{I3} and K_{I4} are shown in Table I and II. The damping ratio δ and oscillatory frequency f_{osc} of each corresponding mode are also listed. Definitions of λ, δ, and f_{osc} are detailed in Appendix B.

Besides $\mathrm{K_{Vi}}$ and $\mathrm{K_{Qi}}$, the relative influences of the other voltage/VAR controller's parameters, such as $\mathrm{K_{iV}}$ and $\mathrm{K_{pV}}$, are calculated and compared in Table III. It is found that the tuning of parameters $\mathrm{K_{Qi}}$ and $\mathrm{K_{pV}}$ have a more obvious impact on the distribution of critical eigenvalues, and thus on the SD voltage stability margin during dynamics.

TABLE I
Eigenvalue Analysis with Different Settings of K_{Vi}
(Base Values: $K_{Vi} = 40, K_{Qi} = 0.1, K_{pV} = 18.0, K_{iV} = 5.0$)

Parameter K_{Vi}	Critical Eigenvalues $\lambda = \sigma \pm j\omega$	Damping Ratio δ	Oscillatory Freq. f_{osc}
20	$0.0570 \pm j4.5221$	-0.0126	0.7197
25	$0.0639 \pm j4.5662$	-0.0140	0.7267
30	$0.0604 \pm j4.6001$	-0.0131	0.7321
40	$0.0429 \pm j4.6444$	-0.0092	0.7392
50	$0.0238 \pm j4.6703$	0.0051	0.7433
60	$0.0077 \pm j4.6845$	0.0017	0.7456
100	$-0.0310 \pm j4.7051$	0.0066	0.7488

TABLE II
Eigenvalue Analysis with Different Settings of K_{Qi}
(Base Values: $K_{Vi} = 40, K_{Qi} = 0.1, K_{pV} = 18.0, K_{iV} = 5.0$)

Parameter K_{Qi}	Critical Eigenvalues $\lambda = \sigma \pm j\omega$	Damping Ratio δ	Oscillatory Freq. f_{osc}
0.01	$0.0285 \pm j4.6410$	-0.0061	0.7386
0.1	$0.0428 \pm j4.6444$	-0.0092	0.7392
0.2	$0.0712 \pm j4.6682$	-0.0152	0.7430
1.0	$1.2252 \pm j7.6439$	-0.1583	1.2166
10	$4.3402 \pm j16.175$	-0.2592	2.5744
20	$3.5500 \pm j21.608$	-0.1621	3.4390
50	$7.3497 \pm j37.370$	-0.1930	5.9477

TABLE III
Summary of Parameters' Relative Influence

	Sensitive Parameters	Insensitive Parameters
$\sigma\ (Eig_{real})$	K_{pV}, K_{Qi}	K_{iV}, K_{Vi}
δ	K_{Qi}	K_{iV}, K_{pV}, K_{Vi}
f_{osc}	K_{iV}, K_{pV}, K_{Qi}	K_{Vi}

From the sensitivity analysis, it is also found that under several cases, the system dominant oscillatory mode is switching from one to another. The consequence of this is that the system dominant state variables will not stay the same. Also, the critical eigenvalues will be switching from one oscillatory mode to another. The critical eigenvalues will map to different modes in the cases when the relatively more sensitive control parameters have been tuned.

C. Case Study in a Large System

To verify the observations summarized in Table III, a 23-bus system is selected as the system to be examined and its single-line diagram is shown in Fig. 10. The system raw data is originally provided by the commercial software PSS/E.

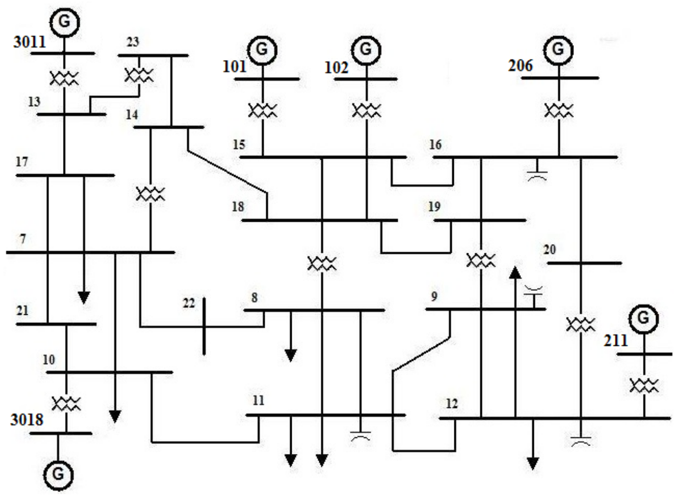

Fig. 10. One-line diagram of the 23-bus System

We will be exploring the SD voltage stability of this system by replacing the generator buses with the collector of DFIWG-based wind farm. Each time only one generator bus will be replaced. The wind generator model used is the GE 3.6 MW DFIG-based WTG. The technical specifications of this model can be found in [17]. In the simulation, to replace the original Bus i generators with a capacity of P_i, a wind farm equipped with $N(=P_i/3.6)$ DFIWGs is assumed.

The parameter sensitivities are calculated at each of the generator buses and shown in Fig. 11. It can be concluded that the observations summarized in Table III holds in most of the cases for this larger system. A different setup of the reactive power controller's parameters with high sensitivities could bring a system from being SD voltage unstable towards being stable.

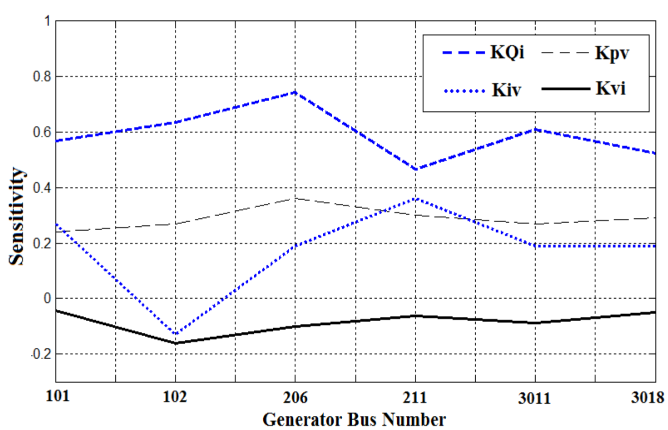

Fig. 11. Parameter sensitivities at each generator bus of the 23-bus system

VI. Conclusions and Future Work

This paper investigates three different yet closely correlated aspects of the voltage stability issue considering grid-connected DFIWG. The conclusions that were reached in this paper include:

- In order to initialize the internal variables, the DFIWG should be integrated in power flow calculations to get a 'snapshot' of current operating point;
- The large disturbance voltage stability considering the actions of mechanical OLTC is studied. Results show that unlike the SCIWG which decreases the voltage stability margin, the DFIWG enables a better voltage performance;
- Small disturbance voltage stability analysis is performed to track the eigenvalue movement with slow variations of wind generation outputs;
- Sensitivity analysis is conducted to quantify the critical eigenvalue variation with respect to the perturbations of DFIWG parameters. It is found that the DFIWG reactive power controller's parameters have considerable impact on the distribution of critical eigenvalue.
- The parameters' relative influence on system small disturbance voltage stability is summarized and verified by extending the sensitivity analysis to a 23-bus system.

In the future work, the parameter sensitivity analysis will be further extended in more detail. Solutions for how to optimize the boundaries of DFIWG parameters, and how it could be applied on-line to increase voltage stability margin based on the synchrophasor measurements will be explored.

VII. Appendix

A. *Settings of the four-bus test system shown in Fig. 4*

Transmission parameters:

$$\dot{E}_{ext} = 1\angle 0^{\circ}, X_{ext} = 0.01, X_l = 0.029,$$
$$X_{24} = 0.012, X_{23} = 0.005$$

Wind generator equivalent model parameters:

$$X_s = 0.1,\ X_r = 0.18,\ X_m = 3.2,\ R_r = 0.018$$

Step-up transformer turns ratio: $n = 1.05$
OLTC transformer turns ratio:

$$n_{min} = 0.80,\ n_{max} = 1.20,\ \Delta n = 0.01$$

Exponential load: $\alpha = \beta = 1.5$

The above values are all in p.u. system. The values are on bases of 120 kV / 100 MVA for transmission system, and on bases of 25 kV / 50 MVA for local wind farm.

B. *Eigenvalue Calculations*

Critical eigenvalues $\lambda = \sigma \pm j\omega$ of the matrix J_L defined in (14) are eigenvalues with the largest participation factor P_{ij}:

$$P_{ij} = \frac{|\Psi_{ji} \cdot \Phi_{ij}|}{\sum_{i=1}^{n} |\Psi_{ji} \cdot \Phi_{ij}|} \qquad (17)$$

where Ψ_{ji} and Φ_{ij} are the ith elements of the left and right eigenvectors of the jth mode. The damping δ and oscillatory frequency f_{osc} are calculated as:

$$\delta = -\frac{\sigma}{\sqrt{\sigma^2 + \omega^2}} \qquad (18)$$

$$f_{osc} = \frac{\omega}{2\pi} \qquad (19)$$

VIII. References

[1] Thierry Van Cutsem and Costas Vournas, *Voltage Stability of Electric Power Systems*, Boston: Kluwer Academic Publishers, 1998

[2] P. Kessel and H. Glavitsch, "Estimating the voltage stability of a power system," *IEEE Trans. Power Delivery*, Vol. 1, Issue 3, 1986
[3] Zbigniew Lubosny, *Wind Turbine Operation in Electric Power Systems*. New York: Springer, 2003
[4] F. Zhou, G. Joos, and C. Abbey, "Voltage stability in weak connection wind farms," IEEE PES General Meeting, 2005
[5] N. R. Ullah and T. Thiringer, "Variable speed wind turbines for power system stability enhancement," *IEEE Trans. Energy Conversion*, Vol. 22, No. 1, pp. 52-60, March 2007
[6] E. Muljadi, C. P. Butterfield, B. Parsons, and A. Ellis, "Effect of variable speed wind turbine generator on stability of a weak grid," *IEEE Trans. Energy Conversion*, Vol. 22, No. 1, March 2007
[7] N. Amjady, and M. R. Ansari, "Small disturbance voltage stability evaluation of power systems," IEEE Transmission and Distribution Conference and Exposition, 2008
[8] Francoise Mei, and Bikash Pal, "Modal analysis of grid-connected doubly fed induction generators," *IEEE Trans. Energy Conversion*, Vol. 22, No. 3, pp. 728-736, Sep. 2007
[9] Hector A. Pulgar-Painemal, and Peter W. Sauer, "Power system modal analysis considering doubly-fed induction generators," IREP Symposium on Bulk Power System Dynamics and Control, August 2010
[10] J. Padron, and A. Lorenzo, "Calculating Steady-State Operating Conditions for Doubly-Fed Induction Generator Wind Turbines," *IEEE Trans. Power Systems*, Vol. 25, No. 2, pp. 922-928, May 2010
[11] Ce Zheng and Mladen Kezunovic, "Distribution System Voltage Stability Analysis with Wind Farms Integration," IEEE PES 42nd North America Power Symposium, Arlington, Texas, USA, September 2010
[12] P. N. Boonchiam, A. Sode-Yome, N. Mithulananthan, and K. Aodsup, "Voltage stability in power network when connected wind farm generators," PEDS, Taipei, Nov. 2009
[13] Vladislav Akhmatov, *Analysis of Dynamic Behavior of Electric Power Systems with Large Amount of Wind Power*. Ph.D. Thesis, Technical University of Denmark, 2003
[14] PTI, PSS/E Application Guide, Vol. I [M], PSS/E Brochure, 2002
[15] P. M. Frank, *Introduction to System Sensitivity Theory*. Academic Press, New York, 1978
[16] I. A. Hiskens and J. Alseddiqui, "Sensitivity, Approximation, and Uncertainty in Power System Dynamic Simulation," *IEEE Trans. Power Systems*, Vol. 21, No. 4, pp. 1808-1820, November 2006
[17] GE Energy, 3.6 MW Wind Turbine Technical Specifications. [Online]. Available: http://www.gepower.com/prod_serv/products/wind_turbines

IX. Biographies

Ce Zheng (S'07) received his B.S. and M.S. degrees from North China Electric Power University, Beijing, China, in 2005, 2007 respectively, all in electric engineering. He has been with Texas A&M University pursuing his Ph.D. degree since August 2007. His research interests include PMU applications, powe system voltage stability, and the integration of renewable energy into power system.

Mladen Kezunovic (S'77-M'80–SM'85–F'99) received the Dipl. Ing., M.S. and Ph.D. degrees in electrical engineering in 1974, 1977 and 1980, respectively. Currently, he is the Eugene E. Webb Professor and Site Director of Power Engineering Research Center (PSerc), an NSF I/UCRC.at Texas A&M University He worked for Westinghouse Electric Corp., Pittsburgh, PA, 1979-1980 and the Energoinvest Company, in Europe 1980-1986, and spent a sabbatical at EdF in Clamart 1999-2000. He was also a Visiting Professor at Washington State University, Pullman, 1986-1987 and The University of Hong Kong, fall of 2007. His main research interests are digital simulators and simulation methods for relay testing as well as application of intelligent methods to power system monitoring, control, and protection. Dr. Kezunovic is a Fellow of the IEEE, member of CIGRE and Registered Professional Engineer in Texas.